

Available online at www.sciencedirect.com**ScienceDirect**

Procedia Engineering 99 (2015) 1358 – 1364

**Procedia
Engineering**www.elsevier.com/locate/procedia

“APISAT2014”, 2014 Asia-Pacific International Symposium on Aerospace Technology,
APISAT2014

Labyrinth Seals Diameter and Length Effect Study on Nonlinear Dynamics

Ma Wensheng^{a,*}, Huang Hai^a, Feng Guoquan^a, Chen Zhaobo^b, R.G Kirk^c

^aAVIC Shenyang Aeroengine Research Institute, Shenyang 110015, China

^bSchool of Mechatronics Engineering, Harbin Institute of Technology, Harbin 15001, China

^cRotor Dynamics Laboratory, Virginia Tech, Blacksburg, VA 24061, USA

Abstract

The stability study has become the most important part of rotor dynamics analysis. In this research, labyrinth seals nonlinear dynamics model is built to evaluate the bifurcation rotor speed of rotor-seals system. It is important to know the accurate bifurcation rotor speed for predicting the instability of rotor-seals system. Labyrinth seals geometric dimension effects on system bifurcation are studied in this paper. Bifurcation rotor speed of rotor-seal system at four seals diameter and four seals lengths are calculated using Runge-Kutta method. The results show that rotor-seals system bifurcation rotor speed will increase with seals diameter and seals length increasing.

© 2015 Published by Elsevier Ltd. This is an open access article under the CC BY-NC-ND license

(<http://creativecommons.org/licenses/by-nc-nd/4.0/>).

Peer-review under responsibility of Chinese Society of Aeronautics and Astronautics (CSAA)

Keywords: Labyrinth seals, nonlinear, dynamics model, Runge-Kutta method

1. Introduction

Rotating machines such as compressors, turbines, pumps, jet engines, turbochargers, etc are subject to rotor-seal system stability. The labyrinth seal has many advantages, such as simplicity, reliability, and tolerance for high temperature and high pressure. The labyrinth seal has improved over the years. Originally, most of the work focused upon experimental data and simplified rotor dynamic systems. Alford[1] studied a labyrinth seals with varying inlet

* Corresponding author. Tel.: +086-159-9830-5799

E-mail address: mawensheng1980@gmail.com

and outlet areas. He concluded that when the inlet area exceeds the outlet area, an excitation force is produced that causes whirl in the direction of the rotation. Conversely, Alford concluded that no excitation force would be produced when the outlet area exceeds the inlet area. Wyss Mann et al.[2,3] used a two control volume approach to model the flow through a labyrinth seals. The two control volume approach is a simplified approach to a finite volume method. For that reason, the modeled flow through the seals was oversimplified and could only be used for general comparisons and trends. Kirk[4] developed a bulk code to determine the dynamic coefficients of a labyrinth seals, the code was called DYNLAB, but recently has been renamed LabyXL. The paper presents a theoretical study of a Jeffcott rotor-seal system. The nonlinear dynamics model of unbalance rotor-seal system is established in this paper. The following results will demonstrate the influence of seals structure on the bifurcation. The comparison bifurcation charts in different parameters of rotor-seal nonlinear system is analyzed in this paper.

2. Labyrinth seals nonlinear dynamics model analysis

Labyrinth seals can be used to reduce leakage from high pressure region into lower pressure region. A rotor-seal system is shown in Fig.1. Then the equations of motion can be written in Eq. (1).

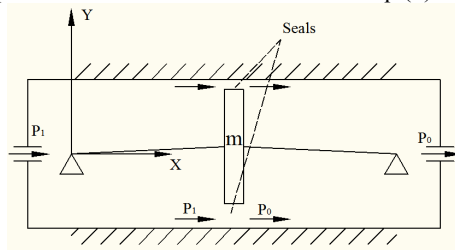


Fig.1 Jeffcott rotor-seal system

Dynamics model:

$$\begin{bmatrix} m & 0 \\ 0 & m \end{bmatrix} \begin{bmatrix} \ddot{x} \\ \ddot{y} \end{bmatrix} + \begin{bmatrix} D_e & 0 \\ 0 & D_e \end{bmatrix} \begin{bmatrix} \dot{x} \\ \dot{y} \end{bmatrix} + \begin{bmatrix} K_e & 0 \\ 0 & K_e \end{bmatrix} \begin{bmatrix} x \\ y \end{bmatrix} = \begin{bmatrix} F_x \\ F_y \end{bmatrix} + \begin{bmatrix} 0 \\ mg \end{bmatrix} + m\omega^2 \begin{bmatrix} \cos\omega t \\ \sin\omega t \end{bmatrix} \quad (1)$$

Muszynska seals model:

$$-\begin{bmatrix} F_x \\ F_y \end{bmatrix} = \begin{bmatrix} K - m_f\tau^2\omega^2 & \tau\omega D \\ -\tau\omega D & K - m_f\tau^2\omega^2 \end{bmatrix} \begin{bmatrix} x \\ y \end{bmatrix} + \begin{bmatrix} D & 2\tau m_f\omega \\ -2\tau m_f\omega & D \end{bmatrix} \begin{bmatrix} \dot{x} \\ \dot{y} \end{bmatrix} + \begin{bmatrix} m_f & \\ & m_f \end{bmatrix} \begin{bmatrix} \ddot{x} \\ \ddot{y} \end{bmatrix} \quad (2)$$

It can get Eq. (3) by Eq. (1) and Eq. (2)

$$\begin{bmatrix} m + m_f & 0 \\ 0 & m + m_f \end{bmatrix} \begin{bmatrix} \ddot{x} \\ \ddot{y} \end{bmatrix} + \begin{bmatrix} D_e + D & 2\tau m_f\omega \\ -2\tau m_f\omega & D_e + D \end{bmatrix} \begin{bmatrix} \dot{x} \\ \dot{y} \end{bmatrix} + \begin{bmatrix} K_e + K - m_f\tau^2\omega^2 & \tau\omega D \\ -\tau\omega D & K_e + K - m_f\tau^2\omega^2 \end{bmatrix} \begin{bmatrix} x \\ y \end{bmatrix} = \begin{bmatrix} 0 + m\omega^2 \cos\omega t \\ mg + m\omega^2 \sin\omega t \end{bmatrix} \quad (3)$$

Define the dimensionless parameters of coordinates: $x = \frac{X}{c}$, $y = \frac{Y}{c}$, $\omega t = \tau$, $\frac{d}{dt} = \omega \frac{d}{d\tau}$, $\frac{d^2}{dt^2} = \omega^2 \frac{d^2}{d\tau^2}$,

$$\dot{x} = \frac{\dot{X}}{c}, \quad \dot{y} = \frac{\dot{Y}}{c}, \quad \ddot{x} = \frac{\ddot{X}}{c}, \quad \ddot{y} = \frac{\ddot{Y}}{c}.$$

Assume $M = m + m_f$, and Eq. (3) become

$$\begin{bmatrix} M & 0 \\ 0 & M \end{bmatrix} \begin{bmatrix} \omega^2 \frac{\ddot{X}}{c} \\ \omega^2 \frac{\ddot{Y}}{c} \end{bmatrix} + \begin{bmatrix} D_e + D & 2\tau m_f\omega \\ -2\tau m_f\omega & D_e + D \end{bmatrix} \begin{bmatrix} \omega \frac{\dot{X}}{c} \\ \omega \frac{\dot{Y}}{c} \end{bmatrix} + \begin{bmatrix} K_e + K - m_f\tau^2\omega^2 & \tau\omega D \\ -\tau\omega D & K_e + K - m_f\tau^2\omega^2 \end{bmatrix} \begin{bmatrix} \frac{X}{c} \\ \frac{Y}{c} \end{bmatrix} = \begin{bmatrix} m\omega^2 \cos\omega t \\ mg + m\omega^2 \sin\omega t \end{bmatrix} \quad (4)$$

$$\begin{bmatrix} 1 & 0 \\ 0 & 1 \end{bmatrix} \begin{bmatrix} \ddot{X} \\ \ddot{Y} \end{bmatrix} + \begin{bmatrix} \frac{D_e + D}{M\omega} & \frac{2\tau m_f}{M} \\ -\frac{2\tau m_f}{M} & \frac{D_e + D}{M\omega} \end{bmatrix} \begin{bmatrix} \dot{X} \\ \dot{Y} \end{bmatrix} + \begin{bmatrix} \frac{K_e + K - m_f \tau^2 \omega^2}{M} & \frac{\tau D}{M\omega} \\ -\frac{\tau D}{M\omega} & \frac{K_e + K - m_f \tau^2 \omega^2}{M} \end{bmatrix} \begin{bmatrix} X \\ Y \end{bmatrix} = \begin{bmatrix} \frac{mcr \cos \omega t}{M} \\ \frac{mcg + mcr \omega^2 \sin \omega t}{M\omega^2} \end{bmatrix} \quad (5)$$

Define the dimensionless parameters:

$$D_1 = \frac{D_e + D}{M\omega}, D_2 = \frac{2\tau m_f}{M}, K_1 = \frac{K_e + K - m_f \tau^2 \omega^2}{M}, K_2 = \frac{\tau D}{M\omega}, G = \frac{cmg}{M\omega^2}, r = \frac{mcr}{M\omega^2} \quad (6)$$

The parameters are into Eq. (6)

$$\begin{bmatrix} 1 & 0 \\ 0 & 1 \end{bmatrix} \begin{bmatrix} \ddot{X} \\ \ddot{Y} \end{bmatrix} + \begin{bmatrix} D_1 & D_2 \\ -D_2 & D_1 \end{bmatrix} \begin{bmatrix} \dot{X} \\ \dot{Y} \end{bmatrix} + \begin{bmatrix} K_1 & K_2 \\ -K_2 & K_1 \end{bmatrix} \begin{bmatrix} X \\ Y \end{bmatrix} = \begin{bmatrix} \rho \cos \omega t \\ G + \rho \sin \omega t \end{bmatrix} \quad (7)$$

Then, Eq. (7) become

$$\begin{bmatrix} \dot{X} \\ \dot{X} \\ \dot{Y} \\ \dot{Y} \end{bmatrix} = \begin{bmatrix} 0 & 1 & 0 & 0 \\ -K_1 & -D_1 & -K_2 & -D_2 \\ 0 & 0 & 0 & 1 \\ K_2 & D_2 & -K_1 & -D_1 \end{bmatrix} \begin{bmatrix} X \\ \dot{X} \\ Y \\ \dot{Y} \end{bmatrix} + \begin{bmatrix} 0 \\ \rho \cos \omega t \\ 0 \\ G + \rho \sin \omega t \end{bmatrix} \quad (8)$$

Assume $x = [x_1 \ x_2 \ x_3 \ x_4]^T = [X \ \dot{X} \ Y \ \dot{Y}]^T$, and $\dot{x} = [\dot{x}_1 \ \dot{x}_2 \ \dot{x}_3 \ \dot{x}_4]^T = [\dot{X} \ \ddot{X} \ \dot{Y} \ \ddot{Y}]^T$

System state equation is obtained from Eq. (8)

$$\begin{bmatrix} \dot{x}_1 \\ \dot{x}_2 \\ \dot{x}_3 \\ \dot{x}_4 \end{bmatrix} = \begin{bmatrix} 0 & 1 & 0 & 0 \\ -K_1 & -D_1 & -K_2 & -D_2 \\ 0 & 0 & 0 & 1 \\ K_2 & D_2 & -K_1 & -D_1 \end{bmatrix} \begin{bmatrix} x_1 \\ x_2 \\ x_3 \\ x_4 \end{bmatrix} + \begin{bmatrix} 0 \\ \rho \cos \omega t \\ 0 \\ G + \rho \sin \omega t \end{bmatrix} \quad (9)$$

Dynamics parameters solution:

$$K = K_0(1 - e^2)^{-n}, D = D_0(1 - e^2)^{-n}, n = \frac{1}{2} \sim 8 \quad (10)$$

$$t = t_0(1 - e^2)^{-b}, 0 < b < 1 \quad (11)$$

$$K_0 = m_3 m_0, D_0 = m_1 m_3 T, m_f = m_2 m_3 T \quad (12)$$

$$m_0 = \frac{2s^2}{1+x+2s} E(1 - m_0) \quad (13)$$

$$\mu_1 = \frac{2\sigma^2}{1+\xi+2\sigma} \left[\frac{E}{\sigma} + \frac{B}{2} \diamond \frac{1}{6} + E \diamond \right] \quad (14)$$

$$m_2 = \frac{s}{1+x+2s} \left(\frac{1}{6} + E \right) \quad (15)$$

$$m_3 = \frac{p R D P}{l} \quad (16)$$

The dynamics parameters, from Eq.(6), Eq. (10) to Eq. (16), are

$$\begin{aligned}
 D_1 &= \frac{D_e + D}{M\omega} \\
 &= \frac{D_e + \frac{2\sigma^2}{1+\xi+2\sigma} \left[\frac{E}{\sigma} + \frac{B}{2} \left(\frac{1}{6} + E \right) \right] \left[\frac{\sigma}{1+\xi+2\sigma} \left(\frac{1}{6} + E \right) \right] T (1-e^2)^{-n}}{\left[m + \frac{\sigma}{1+\xi+2\sigma} \left(\frac{1}{6} + E \right) \right] \left(\frac{\pi R \Delta P}{\lambda} \right) T^2} \omega \\
 D_2 &= \frac{2\tau m_f}{M} = \frac{2\tau_0 (1-e)^b \left[\frac{\sigma}{1+\xi+2\sigma} \left(\frac{1}{6} + E \right) \right] \left(\frac{\pi R \Delta P}{\lambda} \right) T^2}{\left\{ m + \left[\frac{\sigma}{1+\xi+2\sigma} \left(\frac{1}{6} + E \right) \right] \left(\frac{\pi R \Delta P}{\lambda} \right) T^2 \right\}} \\
 K_1 &= \frac{K_e + K - m_f \tau^2 \omega^2}{M} \\
 &= \frac{K_e + \frac{2\sigma^2}{1+\xi+2\sigma} E (1-m_0) \left(\frac{\pi R \Delta P}{\lambda} \right) (1-e^2)^{-n}}{\left\{ m + \left[\frac{\sigma}{1+\xi+2\sigma} \left(\frac{1}{6} + E \right) \right] \left(\frac{\pi R \Delta P}{\lambda} \right) T^2 \right\}} \\
 K_2 &= \frac{\tau D}{M\omega} = \frac{\tau_0 (1-e)^{2b} D_0 (1-e^2)^{-n}}{\left[m + \frac{\sigma}{1+\xi+2\sigma} \left(\frac{1}{6} + E \right) \right] \left(\frac{\pi R \Delta P}{\lambda} \right) T^2} \omega \\
 &\quad - \frac{\left[\frac{\sigma}{1+\xi+2\sigma} \left(\frac{1}{6} + E \right) \right] \left(\frac{\pi R \Delta P}{\lambda} \right) T^2 \tau_0^2 (1-e)^{2b} \omega^2}{\left[m + \frac{\sigma}{1+\xi+2\sigma} \left(\frac{1}{6} + E \right) \right] \left(\frac{\pi R \Delta P}{\lambda} \right) T^2} \omega
 \end{aligned} \tag{17}$$

Where

$$s = \frac{l}{c}, DP = \frac{1}{2} (1+x+2s) v^2 \tag{18}$$

$$\lambda = n_0 R_a^{m_0} \left[1 + \left(\frac{R_v}{R_a} \right)^2 \right]^{\frac{1+m_0}{2}} \tag{19}$$

$$E = \frac{1+z}{1+z+2s}, B = 2 - \frac{\left(R_v / R_a \right)^2 - m_0}{\left(R_v / R_a \right)^2 + 1} \tag{20}$$

$$R_a = \frac{2vd}{m}, R_v = \frac{Rvd}{m} \tag{21}$$

3. Labyrinth seals nonlinear dynamics analysis

The labyrinth seals geometric dimensions are shown in Table 1

Table1 Seals geometric dimensions

Dimensions	Value	Dimensions	Value
Diameter, R	250mm	Gas axial speed, v	30m/s
Radial Clearance, Cr	0.3mm	Inlet loss, ξ	0.1
Seals length, L	76mm	Rotor damp, De	500N/m-sec
Seals mass, m	500kg	Rotor stiffness, Ke	10^7 N/m

3.1. Seals diameter effect study on bifurcation

Fig.2 is the seals diameter effect on rotor-seal system bifurcation. Fig.2 (a) is the bifurcation when the seals diameter is 250mm, rotor-seal system is synchronous motion when rotor speed is less than 545 rad/s. Rotor-seal system is quasi-periodic motion when $545\text{rad/s} < \omega < 601\text{rad/s}$. Rotor-seal system is subsynchronous motion with two-period when $601\text{rad/s} < \omega < 638\text{rad/s}$, and it will become quasi-periodic motion when ω is more than 638rad/s.

Fig.2 (b) is the bifurcation when the seals diameter is 300mm, rotor-seal system is synchronous motion when rotor speed is less than 575 rad/s. Rotor-seal system is quasi-periodic motion when $575\text{rad/s} < \omega < 616\text{rad/s}$. Rotor-seal system is subsynchronous motion with two-period when $616\text{rad/s} < \omega < 660\text{rad/s}$, and it will become quasi-periodic motion when ω is more than 660rad/s.

Fig.2 (c) is the bifurcation when the seals diameter is 350mm, rotor-seal system is synchronous motion when rotor speed is less than 602 rad/s. Rotor-seal system is quasi-periodic motion when $602\text{rad/s} < \omega < 635\text{rad/s}$. Rotor-seal system is subsynchronous motion with two-period when $635\text{rad/s} < \omega < 680\text{rad/s}$, and it will become quasi-periodic motion when ω is more than 680rad/s.

Fig.2 (d) is the bifurcation when the seals diameter is 400mm, rotor-seal system is synchronous motion when rotor speed is less than 617 rad/s. Rotor-seal system is quasi-periodic motion when $617\text{rad/s} < \omega < 652\text{rad/s}$. Rotor-seal system is subsynchronous motion with two-period when $652\text{rad/s} < \omega < 680\text{rad/s}$, and it will become quasi-periodic motion when ω is more than 699rad/s.

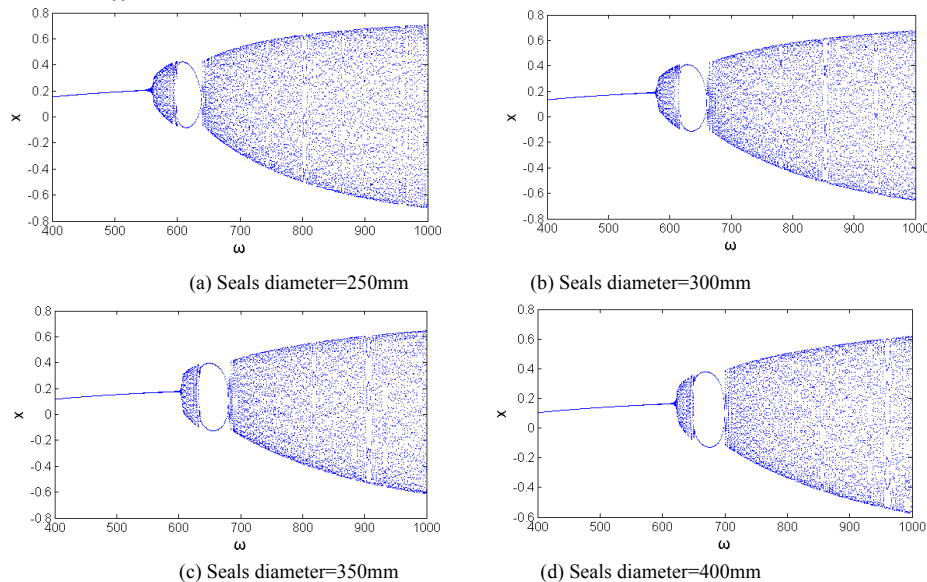


Fig.2 Seals diameter effect study on bifurcation

Table2 Nolinear motion process under different seals diameter

Seals diameter	Nolinear motion process	Speed of quasi-periodic
250mm	SM→APM→DPM→APM	638rad/s
250mm	SM→APM→DPM→APM	660rad/s
250mm	SM→APM→DPM→APM	680rad/s
250mm	SM→APM→DPM→APM	699rad/s

Synchronous motion---SM; Double period motion---DPM; Quasi-periodic motion---APM;

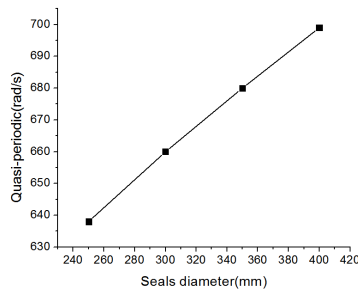


Fig.3 Seals diameter effect study on quasi-periodic motion

3.2. Seals length effect study on bifurcation

Fig.4 is the seals length effect on rotor-seal system bifurcation. Fig.4 (a) is the bifurcation when the seals length is 75mm, rotor-seal system is synchronous motion when rotor speed is less than 557 rad/s. Rotor-seal system is quasi-periodic motion when $557\text{rad/s} < \omega < 600\text{rad/s}$. Rotor-seal system is subsynchronous motion with two-period when $600\text{rad/s} < \omega < 638\text{rad/s}$, and it will become quasi-periodic motion when ω is more than 638rad/s. Fig.4 (b) is the bifurcation when the seals length is 100mm, rotor-seal system is synchronous motion when rotor speed is less than 559 rad/s. Rotor-seal system is quasi-periodic motion when $559\text{rad/s} < \omega < 620\text{rad/s}$. Rotor-seal system is subsynchronous motion with two-period when $620\text{rad/s} < \omega < 660\text{rad/s}$, and it will become quasi-periodic motion when ω is more than 660rad/s. Fig.4 (c) is the bifurcation when the seals length is 150mm, rotor-seal system is synchronous motion when rotor speed is less than 631 rad/s. Rotor-seal system is quasi-periodic motion when $631\text{rad/s} < \omega < 690\text{rad/s}$, and it will become quasi-periodic motion when ω is more than 690rad/s. Fig.4 (d) is the bifurcation when the seals length is 200mm, rotor-seal system is synchronous motion when rotor speed is less than 749 rad/s, and it will become quasi-periodic motion when ω is more than 6749rad/s. From Table 3 and Fig.5, it shows that quasi-periodic rotor speed will increase with the seals length in creasing. Rotor-seal system has not firt quasi-periodic motion when seals diameter is more than 0.075, and it only has synchronous motion and second quasi-periodic motion when seals length is more than 200mm.

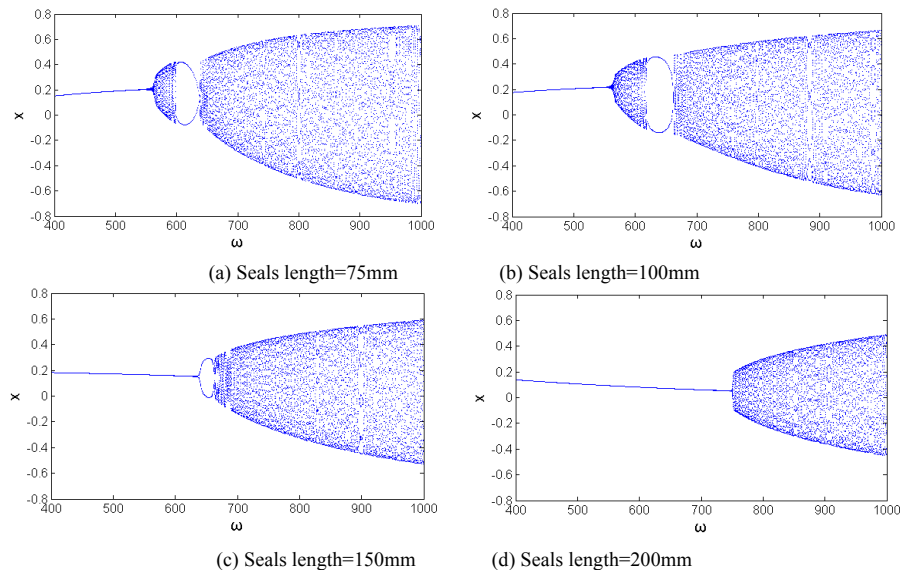


Fig.4 Seals length effect study on bifurcation

Table3 Nolinear motion process under different seals length

Seals length	Nolinear motion process	Speed of quasi-periodic
75mm	SM→APM→DPM→APM	638rad/s
100mm	SM→APM→DPM→APM	660rad/s
150mm	SM-----→DPM→APM	690rad/s
200mm	SM-----→APM	749rad/s

Synchronous motion---SM; Double period motion---DPM; Quasi-periodic motion---APM;

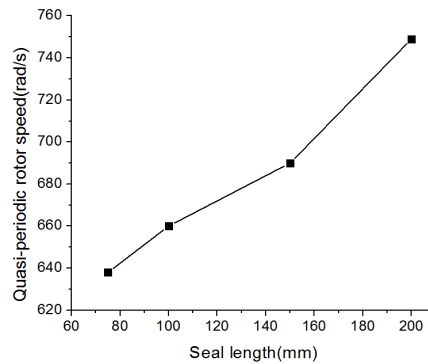


Fig.5 Seals diameter effect study on quasi-periodic motion

4.Conclusions

The paper presents the impact of labyrinth nolinear dynamics motion process by mathematical methods. The study results and discussion give an enhanced cause-effect understanding of pressure effect. It was found that the difference of seals diameter and seals length are important in determining changes of rotor-seal system bifurcation. The rotor speed of quasi-periodic will increase with the seals diameter and seals length increasing. Rotor-seal system is more stability when quasi-periodic rotor speed is greater. The labyrinth seals non-linear dynamics study results have shown that the seals diameter and seals length are beneficial to system stability.

Acknowledgements

This work was supported by the key project of National Nature Science Foundation of China (No.10632040), the project of National Nature Science Foundation of China (No.10872054, No.10872055, No.50905049 and No.11172075).

References

- [1]Alford, J. S (1965). Protecting turbomachinery from self-excited rotor whirl. *Journal of Engineering for Power*, v. 87, 333-334.
- [2]Kirk, R.G (1988). Evaluation of aerodynamic instability mechanisms for centrifugal compressors – part II: advanced analysis. *Journal of Vibration, Acoustics, Stress, and Reliability in Design*, v. 110, 207-212.
- [3]R.G. Kirk and Z.Guo. (2009). Influence of leak path friction on labyrinth seals inlet swirl. *Tribology Society of Tribologists and Lubrication Engineers*(2004), v. 52, 139-145.
- [4]Wyssmann, H.R., Pham T.C., Jenny R.J. (1984). Prediction of stiffness and damping coefficients for centrifugal compressor labyrinth seals. *Journal of Engineering for Gas turbines and Power*, v.106, 920-926.
- [5]Iwatsubo, T. Evaluation of instability force of labyrinth seals in turbines or compressors. *Rotordynamic Instability Problems in High-performance Turbomachinery*. NASA CP No. 2250(1980), proceedings of workshop held at Texas A&M University.
- [6]Childs, D. W. and Scharrer, J. K. An Iwatsubo-based Solution for Labyrinth Seals: Comparison to Experimental Results, *Journal of Engineering for Gas Turbines and Power*(1986), Vol. 108, pp. 325 - 331.